RESEARCH ARTICLE

Quantifying the human disturbance intensity of ecosystems and its natural and socioeconomic driving factors in urban agglomeration in South China

Xiaojun Wang[1] · Guangxu Liu[2] · Aicun Xiang[2] · Salman Qureshi[3] · Tianhang Li[1] · Dezhuo Song[1] · Churan Zhang[1]

Abstract

The impact of human activities on terrestrial ecosystems is becoming more intense than ever in history. Human disturbance analyses play important roles in appropriately managing the human–environment relationship. In this study, a human disturbance index (HDI) that uses land use and land cover data from 1980, 2000, 2010, and 2018 is proposed to assess the human disturbance of ecosystems in the Guangdong-Hong Kong-Macao Greater Bay Area. The HDI is first calculated by classifying the human disturbance intensity into seven levels and 13 categories from weak to strong in ecosystems. Then the driving factors of the HDI spatial pattern change are explored using a geographically weighted regression (GWR) model. The results showed that the spatial pattern of the HDI was high in the middle and low in the surrounding areas. The intensity of human disturbance increased, and the medium and high disturbance areas expanded during 1980–2018, especially in Guangzhou, Foshan, Shenzhen, and Dongguan. Human disturbance displayed an obvious spatial heterogeneity. The GWR model had a better explanation effect of the analysis of the HDI change drivers. The driving effect of the socioeconomic conditions was significantly stronger than that of the natural environmental. This study assists in understanding the distribution and change characteristics of the ecological environment in areas with strong human activities and provides a reference for related studies.

Keywords Ecosystem · Human disturbance · Temporal and spatial characteristics · Geographically weighted regression (GWR) · Guangdong-Hong Kong-Macao Greater Bay Area (GHMGBA) · Urban agglomeration

Introduction

Land covers are the geographic landscapes formed by natural environmental conditions, but they are influenced and modified by human activities (Gu et al. 2007; Li et al. 2018). During the

interaction between humans and the environment, the surface landscape is affected intentionally or unintentionally in both natural and urban areas (Ren et al. 2014; Feng et al. 2018). Rapid urban expansion has driven land cover changes across various terrains (Wu et al. 2015; Dai et al. 2018a; Mansour et al. 2020). The reduction of the adverse effects of land cover change on the urban climate (Arsiso et al. 2018), ecosystems (Peng et al. 2017), human settlement environments (Asabere et al. 2020), and other aspects has become an important challenge for regional sustainable development. Therefore, quantitative assessments of the human activity intensity in different regions are critical for correctly handling the relationship between humans and the environment. This assessment plays a vital role in optimizing the development of land resources, understanding the current situation of the ecological environment, and implementing ecological restoration, especially in areas with intense land use and cover changes.

Human disturbance, which can also be referred to as hemeroby, was an idea proposed by Jalas in 1955 to quantify the impact of human activities on vegetation (Jalas 1955;

Responsible Editor: Philippe Garrigues

✉ Xiaojun Wang
gwangxj@163.com

✉ Guangxu Liu
lg760411@126.com

1   School of Geography Sciences, South China Normal University, Guangzhou 510631, China

2   School of Geography and Environmental Engineering, Gannan Normal University, Ganzhou 341000, China

3   Institute of Geography, Humboldt University of Berlin, Rudower Chaussee 16, 12489 Berlin, Germany

Walz and Stein 2014). Sukopp (1976) defined the degree of hemeroby to assess the impact of human activities on ecosystems. His basic idea was to use the habitat index to classify ecosystems into undisturbed, partially disturbed, and anthropogenically dominated. Other researchers have referred to this idea to clarify the impact of human activities on the surface environment (Hannah et al. 1994), and to quantify anthropogenic disturbance to animal food sources during land development (Gill et al. 1996). In addition, it has been used to specifically analyze the impact on creatures and their habitats due to artificial facilities such as roads, human hunting, just passing through animal territories, and land use changes (Kerley et al. 2002; Stankowich 2008; de Matos et al. 2021). It has also been used to explore the pronounced changes in biological land use in urban human settlement environments (Markovchick-Nicholls et al. 2008). Human disturbances are closely related to landscape patterns and vulnerability (Evans et al. 2017; Shi et al. 2020), and these disturbances are reflected as land use changes that can impact environmental conditions (Wang et al. 2013). With progress in surface information extraction technologies, land cover is becoming increasingly refined, and this helps to distinguish the differences between natural and anthropogenic landscape and identify landscapes types at different spatial scales. Therefore, quantifying the intensity of human activities through land cover types has become a popular research field.

Several studies have investigated land use development intensities and have quantified human activities. Roth et al. (2016) found that human disturbances increased in Mexico from 2002 to 2013, but the growth rate slowed down significantly during 2002–2008 and 2008–2013. Ning et al. (2015) discovered that human disturbances to ecosystems in China showed an upward trend from 1990 to 2010, with a higher level in the northeast and northern China. Similar trends have been found in other studies. The coastal zone, containing wetland ecosystems, has been found to be degraded in the landscape and the intensity of anthropogenic disturbance has gradually increased in the coastal areas of Jiangsu in recent decades (Zhou et al. 2018; Cui et al. 2021). Port construction and beach reclamation were important reasons behind this phenomenon (Zhou et al. 2018). In Shenzhen in South China, where there is also a coastal area, it was found that human disturbance changed significantly (Yi et al. 2020). The primary factors for this change might have been related to the coastal geomorphology (Yi et al. 2020). The population density, gross domestic product (GDP), and topography are important factors in hilly areas that affect human disturbance and ecosystem service values (Chen et al. 2020). The expansion of construction land and cultivated land reclamation has caused human disturbance changes and landscape fragmentation in Daqing (Tian et al. 2020). A certain internal relationship between human disturbance and ecological vulnerability was found in Qiqihar, another city in Northeast China (Yang and Song 2021).

These studies provide references for relevant studies performed in different regions. In addition, there are differences in the distribution and driving factors of human disturbance in a variety of environments. It has been demonstrated that it is of great significance to clarify the role of the natural environment and socioeconomic factors on the intensity of human disturbance. However, this is an aspect that still requires further study, especially in areas with intense land use and cover changes.

The Guangdong-Hong Kong-Macao Greater Bay Area (GHMGBA) is one of the most economically concentrated and developed areas in South China. This region is characterized by megacities with dense populations, as well as busy transportation and a high GDP. Accordingly, issues such as spatial and temporal characteristics and drivers of land use change, especially urban expansion (Jiao et al. 2019; Feng et al. 2021; Dai et al. 2018b; Zhang et al. 2020), urban heat island patterns and anthropogenic heat emissions (Yu et al. 2019; Ma et al. 2021; Peng et al. 2021), changes in ecosystem service values (Zhou et al. 2019; Xu and Zhang 2021), and regional ecological security patterns (Bi et al. 2020; Li et al. 2020a; Wang et al. 2020a), have gradually come to the forefront of attention. In such a typical urban region, the impact of human activities on the surface environment cannot be ignored. Therefore, in this study, a human disturbance index is proposed to quantitatively assess the intensity of human activities of the surface ecological environment in the GHMGBA. There are three specific aims this study, which are as follows: first, to investigate and quantify the disturbance intensity of terrestrial ecosystems in the GHMGBA from 1980 to 2018; second, to describe the spatial and temporal characteristics of the human disturbance intensity and its change trends; third, to analyze the influence of both the natural environmental and socioeconomic factors on the human disturbance intensity.

Materials and methods

Study area

The GHMGBA is composed of the former Pearl River Delta Urban Agglomeration, Hong Kong, and Macao and is located in the Pearl River Delta in the central of Guangdong Province of South China (21°27′N–24°24′N, 111°21′E–115°28′E) (Figure 1). The area is characterized by flat terrain, abundant water resources, sufficient light and heat, and excellent climatic conditions. The average annual temperature ranges between 21.4 and 22.4°C, and the average annual rainfall is 1800 mm. It is influenced by a typical subtropical monsoon climate, with concentrated rainfall from April to September. Owing to its unique land and sea location, it often suffers from typhoons, rainstorms, and other climate disasters. The vegetation type is primarily subtropical evergreen broad-leaf forests with some
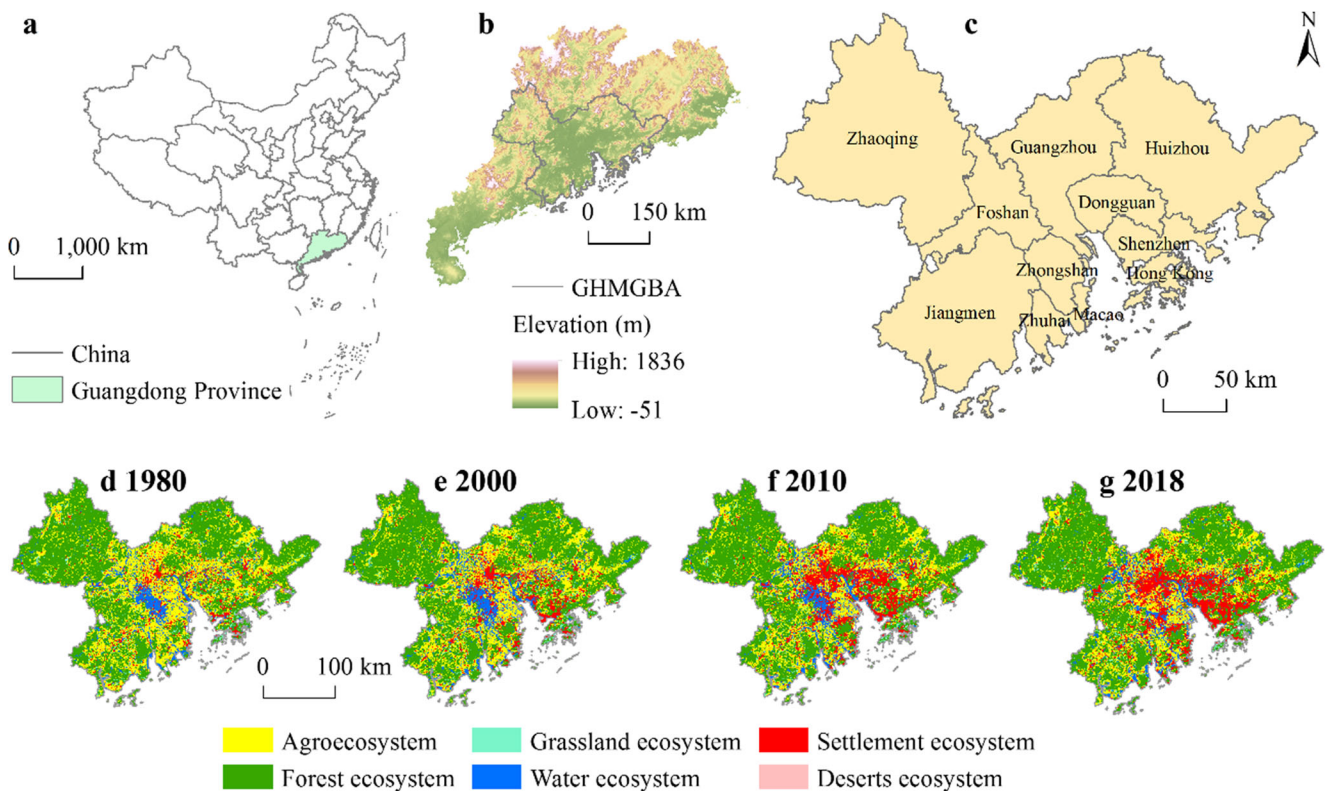
Fig. 1 Location (a–c) and ecosystem distribution (d–g) of the GHMGBA. The GHMGBA refers to the Guangdong, Hong Kong, and Macao Bay Area (the same below). The ecosystem distribution was obtained from the LUCC data

tropical plants. In addition, mangroves are found along the coastal areas. The GHMGBA contains 11 cities with differences in their comprehensive carrying capacities (Weng et al. 2020). The total area is approximately 5.6×10^4 km², accounting for 31.16% of Guangdong Province. At the end of 2018, the total population exceeded 70 million, accounting for more than 60% of the total population in the entire province. In 2019, the GDP was 11.59 trillion yuan (CNY), in which Shenzhen, Hong Kong, Guangzhou, and Foshan exceeded one trillion yuan. The goal of leaders in this area is to become one of the four great bay areas in the world, like New York Bay Area, San Francisco Bay Area in the USA, and Tokyo Bay Area in Japan. From 1980 to 2018, the forest ecosystem was dominant in this region, but the settlement ecosystem has expanded markedly (Figure 1d–g). With continuous social improvements and economic development, the GHMGBA will produce an increasing disturbance to the natural ecological environment.

Research framework and data

The research framework shows the plan to achieve the goal of investigating the spatial pattern and driving mechanism of human disturbance of ecosystem in the GHMGBA (Figure 2). First, based on land use data, the ecosystem was classified into human disturbance

using the disturbance grade standard, and the different ecosystems in the region were integrated into the human disturbance index (Table 1). Second, the representative indicators were selected from the natural environment and social economy, and the influencing factors of the human disturbance spatial heterogeneity were screened and analyzed using a correlation analysis and a principal component analysis. Third, the driving mechanism of the natural environment and socioeconomic factors on the spatial heterogeneity of human disturbance change were analyzed based on ordinary least squares and geographically weighted regression model.

Multiple data from six sources were required according to the study objectives and framework (Table 2). The land use and cover change (LUCC) types were reclassified into six types including cultivated land, forest land, grassland, water area, construction land, and unused land. The six following ecosystems, farmland ecosystems, forest ecosystems, grassland ecosystems, water ecosystems, settlement ecosystems, and desert ecosystems, were reclassified using the LUCC data according to the *Classification and Coding of Terrestrial Ecosystems in China* guidelines (http://www.resdc.cn/) (Figure 1d–g). Five datasets from the natural environment and social economy were used to analyze the driving forces of the HDI. Among them, the linear densities of the roads and rivers (1 km×1 km) were calculated using ArcGIS.

Table 1 Classification of the human disturbance in the ecosystems based on the LUCC

Classification	Land cover types	Ecosystem type	Disturbance intensity
H1, no	Permanent glacier snow	Water ecosystem	1
H2, weak	Woodland	Forest ecosystem	2
	High-coverage grassland	Grassland ecosystem	
	Sandy land, Gobi, saline land, bare land, stone texture, desert	Desert ecosystem	
H3, mild	Shrubland, sparse woodland	Forest ecosystem	3
	Medium-coverage grassland	Grassland ecosystem	
	Lakes, seas, beaches, swamps	Water ecosystem	
H4, medium	Low-coverage grassland	Grassland ecosystem	4
	Canals, reservoirs, and ponds	Water ecosystem	
H5, severe	Paddy field, dry land	Farmland ecosystem	5
	Garden plot	Forest ecosystem	
H6, very severe	Factories and mines, industrial areas, saltworks, etc.	Settlement ecosystem	6
H7, complete	Urban land, rural residential areas	Settlement ecosystem	7

Human disturbance intensity

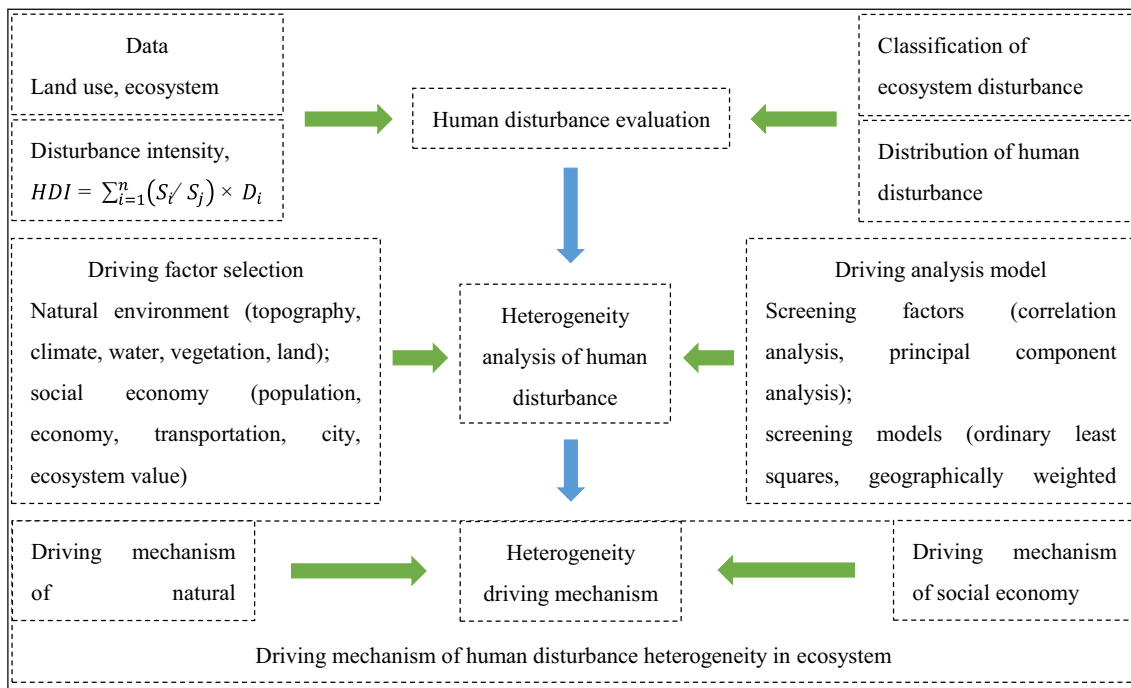### Human disturbance index (HDI)

Human disturbance has changed land use patterns and ecological processes, and different land use types reflect different human development and utilization intensities (Wang and Liao 2006; Liang and Liu 2011; Hou et al. 2019). A human disturbance index (HDI) model based on the area proportions of the different land use types was proposed to evaluate the disturbance intensity of the ecosystem affected by human activities in the GHMGBA from 1980 to 1980. The primary concept was obtained from the comprehensive index model of the land use degree (Zhuang and

Liu 1997; Hou et al. 2019) that establishes a quantitative relationship between human activities and the ecological environment with land use remote sensing monitoring data (Zhai et al. 2018). The equation is as follows:

$$HDI = \sum_{i=1}^{n} \left(S_i / S_j \right) \times D_i \qquad (1)$$

where n is the number of ecosystem types with different disturbance levels, and the maximum value of n in this study was 13; S_i is the area of the ith ecosystem type in the sampling grid (km^2); S_j is the total area of the sampling grid (km^2); and D_i is the disturbance intensity coefficient reflected by the ith ecosystem type (Table 1).

Fig. 2 Framework of the spatial pattern and driving mechanism of human disturbance in the ecosystem

Table 2 Data sources

Data	Sources
LUCC (1980, 2000, 2010, 2018, 1km)	National Earth System Science Data Center (http://www.geodata.cn/)
DEM (250m×250m)	Geospatial Data Cloud (https://www.gscloud.cn)
Meteorological data (1980–2015, 1km)	China Meteorological Data Service Centre (http://data.cma.cn)
Water system and roads	Open Street Map (https://www.openstreetmap.org)
NDVI (2015, 1km), farmland potential productivity (2010), population density, the GDP density (2015), the ecosystem service values (2015)	Resource and Environmental Science Data Center (http://www.resdc.cn/)
Night light (2017, 1 km × 1 km)	Geography Resource and Ecology Knowledge Service System (http://geo.ckcest.cn)

With reference to the following studies (Feng et al. 2017; Guo et al. 2018; Hou et al. 2019), the intensity of ecosystem disturbance was divided into seven levels. Different disturbance levels exist in the same ecosystem category. For example, within the "Forest ecosystem" classification, there are the difference disturbance levels of "Woodland," "Shrubland," and "Garden plot," which were classified into different categories. Therefore, 13 categories under seven disturbance levels were defined, of which there were at least two categories of ecosystems at each level of disturbance levels H2–H5 (Table 1). The ecological system and data had a resolution of 1 km × 1 km, which was resampled into a 5 km × 5 km resolution for the grid analysis to assess the degrees of human disturbance during 1980, 2000, 2010, and 2018. The results were then assigned to the grid center to form a point set, and this was interpolated using the inverse distance weighting (IDW) method to obtain the spatial distribution.

Measuring geographical distributions

The center element, displacement distance, and direction distribution are good indicators to describe the change characteristics of the human disturbance intensity, and they were obtained using ArcGIS For the central elements and displacement distance, the basic idea was to find points with the smallest distances from all the elements that showed the most centrally located element in an area, and then the distance was calculated. The directional distribution was expressed using the standard deviation ellipse, which reflects the spatial characteristics of geographic elements such as the central tendency, the dispersion, and directional trends.

Spatial pattern driving factor analysis

Driving factor selection

The driving mechanism of the HDI spatial pattern was analyzed using the changes in the HDI from 1980 to 2018 as the dependent variable Y, and the 16 factors from the natural environment and social economy were used as the drivers of the independent variable X (Table 3). The natural environmental factors involved topographic relief, climate, water resources, vegetation, and land use. The socioeconomic factors involved population, economy, urban development, and the transportation distribution.

Geographically weighted regression model

The geographically weighted regression (GWR) model is a powerful tool used to explore the heterogeneity of spatial relationships (Propastin 2012). As a local spatial regression model, the GWR model considers the spatial location attribute of data, and this effectively solves the non-stationarity of variable space (Fotheringham et al. 1998). The GWR model has been applied in many disciplines and has shown a higher accuracy than conventional regression models, such as the ordinary least squares (OLS) model (Wang et al. 2020b; Xu et al. 2021; Liu et al. 2021a). It is also widely used for the spatial analysis of geographical elements, such as analyzing the relationship between ecosystem service values and land use (Wang et al. 2018), identifying temporal and spatial dynamics of pollutants (Guo et al. 2021; Pei et al. 2021), estimating surface temperature changes (Qin et al. 2021), and other factors. The calculation method is as follows (Wang et al. 2020b; Xu et al. 2021; Liu et al. 2021a):

$$y_i = \beta_0(\mu_i, v_i) + \sum_{j=1}^{k} \beta_j x_{ij} + \varepsilon_i \tag{2}$$

where y_i and x_{ij} are the results of the dependent variable (the HDI in an ecosystem), y, and the explanatory variable (driving factor), x, at position (u_i, v_i); the coefficients, $\beta_j(u_i, v_i)$ (j=1, 2, … k), are k functions on the spatial location; and ε_i (i=1, 2, ..., k) is an error with a mean variance of σ^2. The model parameters, $\beta_j(u_i, v_i)$ (j=1, 2, ..., k), are location dependent and are typically estimated locally using a weighted least squares approach.

Table 3 Driving factors of the human disturbance spatial pattern

Factor	Resolution	Time	Factor	Resolution	Time
D11: Elevation (m)	250 m	-	D21: Population density (person/km^2)	1 km	2015
D12: Slope (°)	250 m	-	D22:GDP density (10^4 yuan/km^2)	1 km	2015
D13: Annual temperature (°C)	1 km	1980–2015	D23: Proportion of urban land (%)	1 km	2018
D14: Annual precipitation (mm)	1 km	1980–2015	D24: Night light index	1 km	2017
D15: Drainage density (km/km^2)	1 km	-	D25: Traffic density (km/km^2)	1 km	2018
D16: Distance from water body (m)	1 km	-	D26: Ecosystem service value (CNY/hm^2)	1 km	2015
D17: NDVI	1 km	2018	D27: Distance from city (m)	1km	-
D18: Farmland potential productivity (kg/ha)	1 km	2010	D28: Distance from road (m)	1 km	2018

The performance of the GWR model is sensitive to the spatial kernel function and bandwidth statistics methods. To verify the reliability and accuracy of the model, a set of evaluation parameters were calculated based on ArcGIS 10.2. These included the coefficient of determination (R^2), the corrected Akaike information criterion (AICc), standardized residuals, the variance inflation factor (VIF), and the F-test. A larger R^2 signifies a better fit. The smaller the F-test, the better the AICc. In addition, the VIF should be less than 7.5.

The GWR model requires less linear characteristics in the independent variables to avoid data redundancy. A correlation analysis (CA) is a method used to describe the correlation degree between objective matters using appropriate statistical indicators (Gogtay and Thatte 2017). In addition, it has been used to study land use change (Hou and Wen 2020). However, only the use of a CA may lead to a lack of information or even directly discarding a factor because the spatial heterogeneity covers different geographic information symbols that might show linear characteristics when measured. Hence, a principal component analysis (PCA) was used in this study to extract the new variables principal component, 1–n (PC1–PCn). PC1–PCn, without data redundancy, which decrease in the order of the percentage of variance, are able to express the ability of human activity to disrupt ecosystems and are maximally independent between each other (Abdi and Williams 2010). A PCA has the advantages of data dimension reduction and is widely used in the analysis of land use driving factors (Leśniewska-Napierała et al. 2019), air quality (Guo et al. 2021), environmental pollution (Li et al. 2020b), the extraction of the remote sensing ecological index (Qureshi et al. 2020), and other fields.

Results

Classification of the HDI in the ecosystem

The GHMGBA had 6 levels and 12 categories according to the spatial distribution classification of the HDI in the ecosystem from 1980 to 2018 (Figure 3). Weakly disturbed ecosystems like forests, grasslands, and deserts are primarily distributed in Zhaoqing, Yangjiang, and Huizhou, and these areas had weak HDI levels, with the area proportion reaching 45.87–47.5%. Mildly disturbed ecosystems, such as forests, grasslands, and water ecosystems, were scattered and fragmented, with an area proportion of 6.67–8.46% in the transition zone from the weak HDI disturbed levels to the medium and severe levels. The medium disturbed HDI level from grasslands and water ecosystems, primarily rivers, were distributed in low-lying beach areas, especially in the Pearl River Delta region, with an area proportion of 6–7.5%. The severely disturbed HDI, such as farmlands and forest ecosystems, were distributed in flat areas and transition zones. These areas are easily disturbed from human activities and can be easily divided by other types of ecosystems, but maintain small concentrated areas. The severely disturbed HDI levels accounted for 25.9–32.5%. The very severely distributed HDI levels, such as settlement ecosystems, accounted for only 0.6–3.58%, which was the lowest area proportion of all the ecosystems. The completely disturbed HDI levels of the settlement ecosystems were distributed in the middle of the GHMGBA, in the delta, and along the coastal areas, with a proportion of 4.93–11.29%.

Temporal and spatial characteristics of the HDI

Temporal and spatial distribution of the HDI

The temporal and spatial distribution of human disturbance in the ecosystems from 1980 to 2018 showed that human disturbance in the GHMGBA was high in the middle and low at the periphery (Figure 4). The human disturbance was low (2–3.5) in Zhaoqing, Yangjiang, and Huizhou, but high (5.5–7) in Guangzhou, Foshan, Zhongshan, and Dongguan. The human disturbance areas were quite different between Shenzhen and Hong Kong.

The area proportions with HDIs of 2–2.5, 2.5–3.5, and 3.5–4.5 were continuously decreasing during 1980–2018, and they
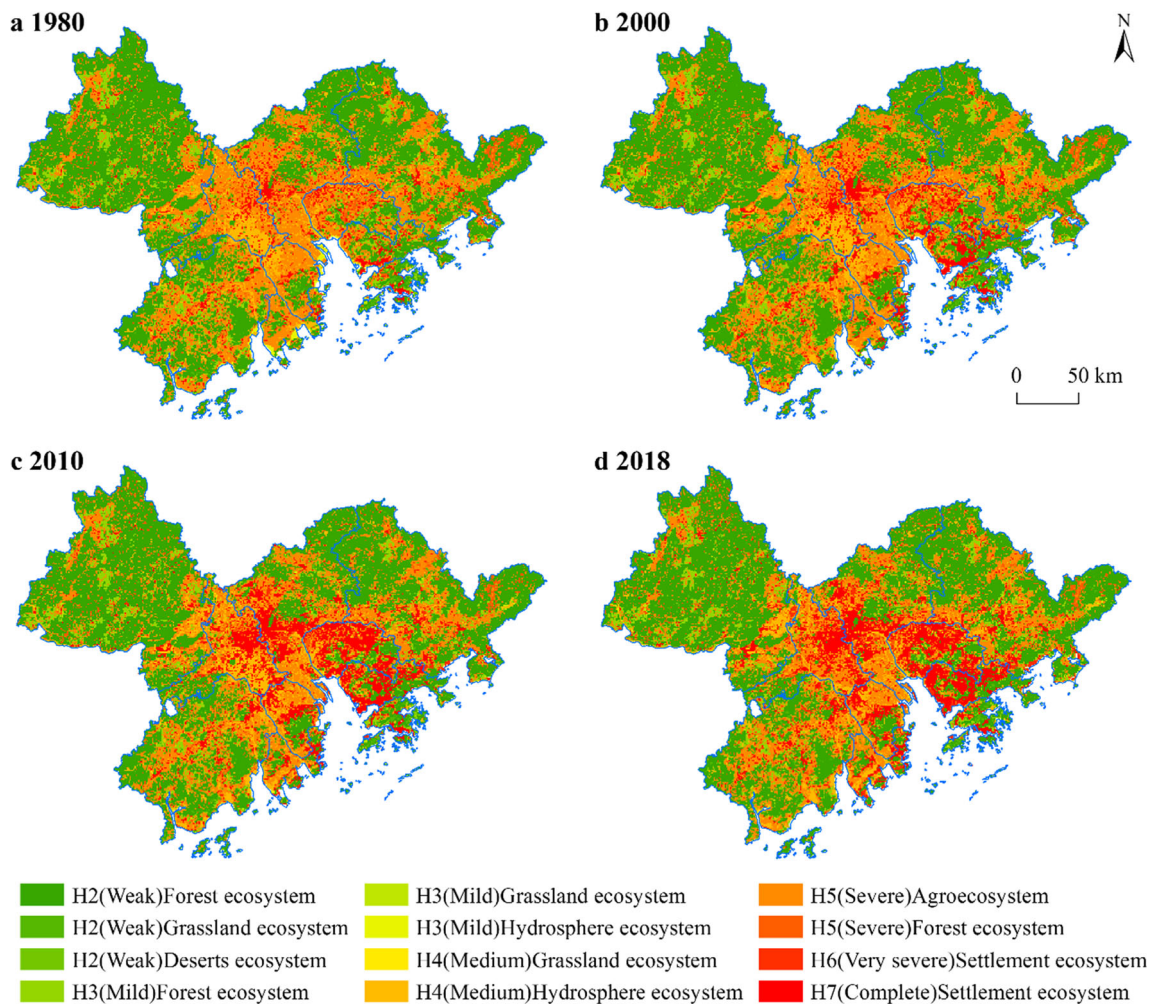
Fig. 3 Classification of the human disturbances in the ecosystems of the GHMGBA from 1980 to 2018. There are different color symbols for the same disturbance levels. These are due to the different ecosystem types

were 15.47%, 3.91%, and 13.51% during 1980–2000, 200–2010, and 2010–2018, respectively. The HDI of 4.5–5.5 changed slightly in area. The area with HDIs of 5.5–6.5 and 6.5–7 increased rapidly from 1980 to 2018, from 462 to 4811 km² and 5 to 427 km², respectively. The regions with HDIs greater than 5.5 expanded significantly in Foshan, Guangzhou, Dongguan, and Shenzhen (Figure 4).

Central elements and displacement of the HDI

The distribution and displacement of the HDI center elements quantitatively express the distribution and changes of each level during the different times, reflecting the distribution and changes in human activity intensities in the GHMGBA (Figure 5). The HDI of 2–2.49 (Figure 5b), primarily distributed in Zhaoqing, northwest of the GHMGBA, moved 5656.85 m northeast, 15033.3 m southeast, and 20223.75 m during 1980–2000, 2000–2010, and 2010–2018, respectively. Figure 5b shows the larger displacement angles and distances. The HDI of 2.5–3.49 (Figure 5c), also primarily distributed in

Zhaoqing, moved 1000 m south, 15811.39 m northwest, and 4000 m south during each period, respectively, but with smaller displacement angles. The larger displacement distances occurred in 2000–2010. The HDI of 3.5–4.49 (Figure 5d), primarily distributed in Foshan, the central part of the GHMGBA, has moved southwest since 1980, with a larger displacement angle. It had displacement distances of 0 m, 5099.02 m, and 5099.02 m during the three periods.

The HDI of 4.5–5.49 (Figure 5e), primarily distributed in Guangzhou, moved 7071.07 m southeast, 5385.16 m southwest, and 3162.28 m southeast during the three studied periods of 1980–2000, 2000–2010, and 2010–2018, respectively. In addition, the displacement distances were relatively shorter. The HDI of 5.5–6.49 (Figure 5f) that was first distributed in Guangzhou moved to Dongguan in 2010 and finally back to Guangzhou, and moved 10,049.88 m southeast, 32,015.62 m southeast, and 16,492.42 m southwest during the three periods, with larger displacement angles and distances. The HDI of 6.5–7 (Figure 5g) was first distributed in Zhuhai, then in Guangzhou and Foshan, and it moved
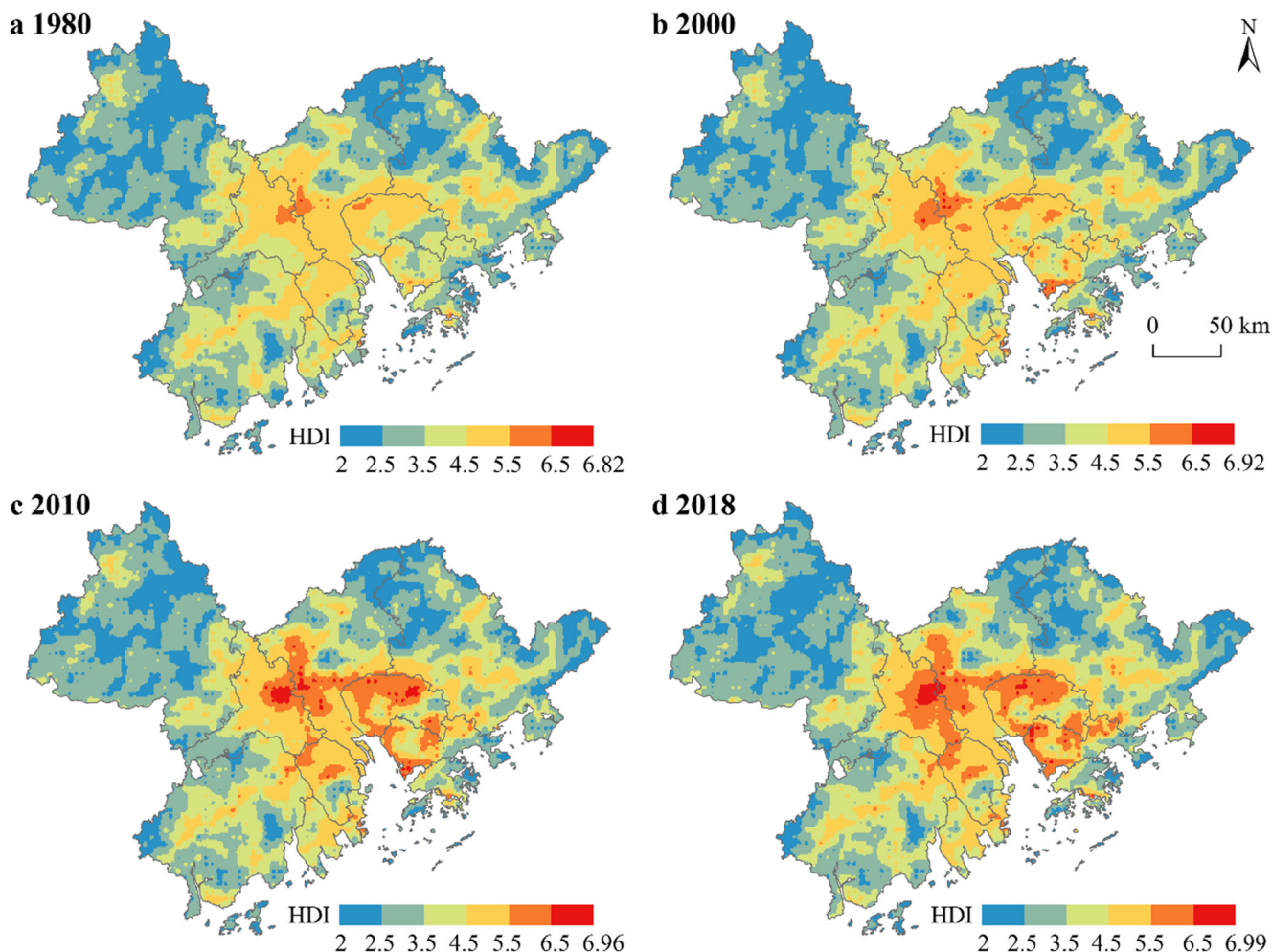
Fig. 4 Distribution of the human disturbances in the ecosystems of the GHMGBA from 1980 to 2018

107,154.09 m northwest, 3,162.28 m southwest, and 5,830.95 m southwest, with large displacement distances during 1980–2000.

Concentration and direction characteristics of the HDI

The ellipse distribution of the standard deviation of the HDI was calculated to characterize the concentration and direction of the HDI. The standard deviation ellipse changed from high (4.5–7) HDI areas more than low (2–4.49) in 1980, 2000, 2010, and 2018, and there were great differences in the HDI standard deviation ellipse in the transition period during 1980–2000, 2000–2010, 2010–2018, and 1980–2018 (Figure 6, Table 4). The standard deviation ellipse of the four years displayed small differences in the areas with the low HDIs (Figure 6a, Table 4). The low and medium HDIs were located primarily in the peripheral areas of the GHMGBA, with an obvious east-west distribution direction. The centripetal force and directionality of the disturbance degree were obvious. The low and medium HDIs slowly moved to Zhaoqing and other areas in the northwest.

The standard deviation ellipse of the high HDI exhibited a certain difference (Figure 6b, Table 4), but the variation was small. The medium-high HDI had a southwest-northeast direction in the GHMGBA ecosystem. The centripetal force and directionality were not as obvious as those in the middle and low areas. The medium-high disturbances were concentrated in central Guangzhou, Foshan, Dongguan, Shenzhen, and Zhongshan. There was a development trend toward the southeast in Dongguan and Shenzhen.

The standard deviation ellipse and its information were quite different during the three transitional periods of 1980–2000, 2000–2010, and 2010–2018 (Figure 6c, Table 4). The overall standard deviation ellipse during 1980–2018 was between that of 2000–2010 and 2010–2018, and closer to that of 2010–2018. These findings indicated that the distribution of the HDI showed a northwest-southeast trend first and then near east-west. The HDI enhancement expanded and developed to the west and north, which was consistent with the information in Figure 4.
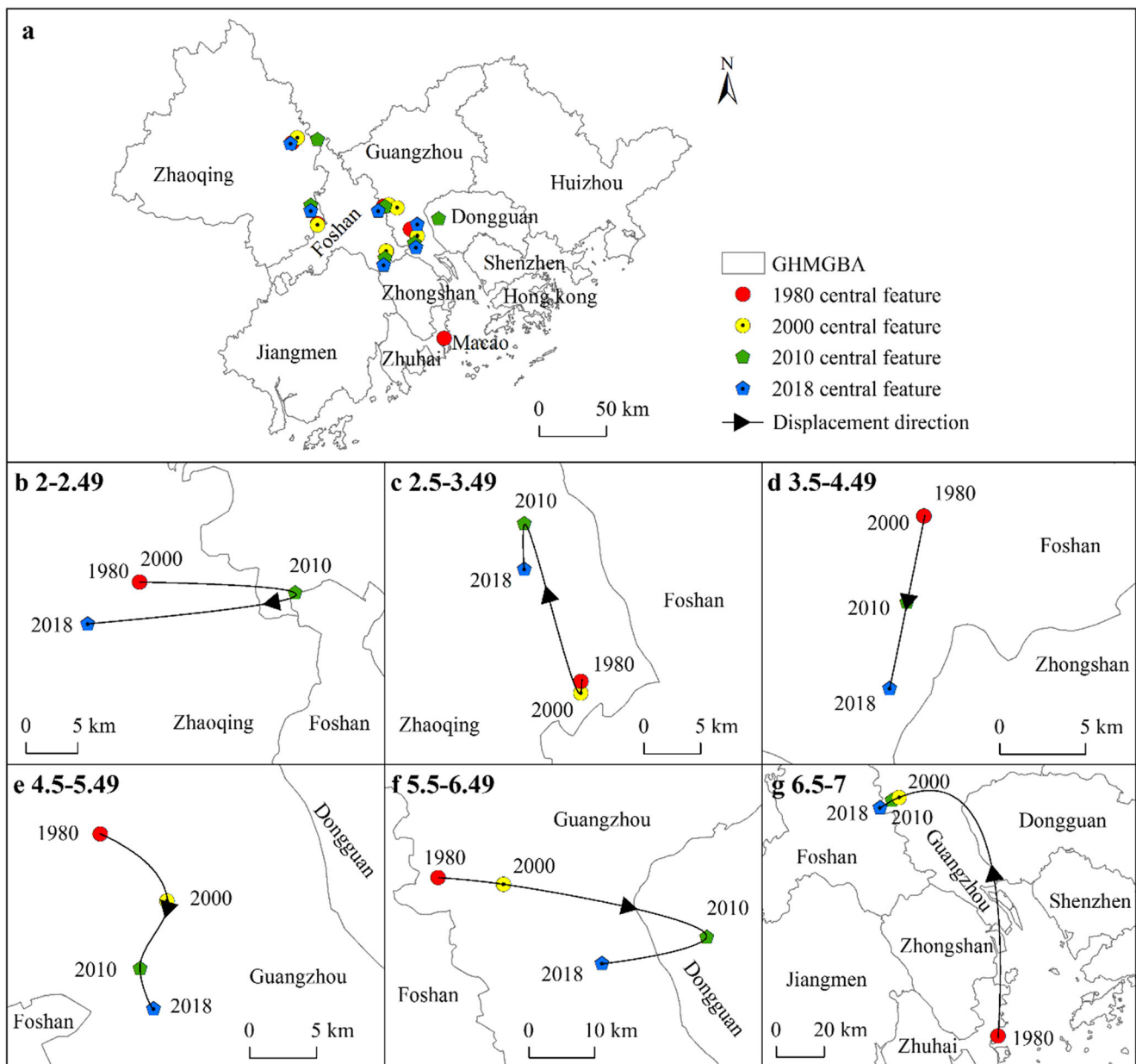
Fig. 5 Displacement of the centers of the HDI in the different levels in the ecosystem of the GHMGBA from 1980 to 2018

Driving factor selections of the HDI spatial pattern

The results of the correlation analysis

The CA results showed that the factors had correlations with the HDI both in the natural environments and in the social environments (Figure 7). The topographic factors were positively related to the NDVI and farmland potential productivity. The temperature was negatively related to the topographic factors and the DNVI. The population, GDP, urban, and traffic factors were positively related to each other, but they were negatively related to the distances from cities and roads. These findings indicated that the selected factors had redundant numerical messages. Therefore, the PCA was used to extract the required information.

The results of the principal component analysis

Three principal component factors from the natural environment (PC-Nat) and two from the social economy (PC-Soc) were extracted using a principal component analysis (PCA) with eigenvalues greater than one as the threshold value. The variance percentages of the PC-Nat 1, 2, and 3 were 48.05%, 15.11%, and 12.67%, respectively. Their cumulative information amounted to 75.82%. The variance percentages of the PC-Soc 1 and 2 were 54.45% and 14.704%, respectively.

Table 4 Parameters of the HDI standard deviation ellipse in the ecosystems of the GHMGBA from 1980 to 2018

Year		Major axis (km)	Minor axis (km)	Axis difference (km)	Rotation (°)	Perimeter (km)	Area (km²)
	1980	146.89	95.39	51.5	88.93	769.75	44015.62
HDI	2000	147.8	95.86	51.94	88.08	774.20	44508.44
2–4.49	2010	149.66	97.41	52.25	87.53	784.89	45797.34
	2018	150.48	97.73	52.75	87.26	788.59	46198.58
	1980	75.83	55.05	20.78	67.72	413.78	13115.14
HDI	2000	76.36	56.45	19.91	73.01	419.56	13540.11
4.5–7	2010	77.07	55.97	21.1	78.57	420.58	13550.55
	2018	77.87	55.75	22.12	78.76	422.63	13636.08
1980–2000		100.19	63.96	36.23	99.59	521.98	20129.46
2000–2010		120.61	72.14	48.47	100.13	615.13	27331.89
2010–2018		127.84	88.89	38.95	87.70	686.36	35696.99
1980–2018		125.57	85.8	39.77	93.25	669.90	33843.02

Their cumulative information amounted to 69.16%. The principal component coefficient matrix (Table 5) shows the different impact factor coefficients extracted from the five principal components, from which new variables can be created.

Among the natural environmental factors, PC-Nat 1 indicated the topography, temperature, and farmland potential productivity. PC-Nat 2 indicated the water resources and vegetation conditions, and PC-Nat 3 indicated the precipitation and farmland potential productivity. Among the socioeconomic factors, PC-Soc1 indicated the population, economy, and cities. PC-Soc2 indicated the ecosystem service value and distances to cities and roads.

Evaluation model of the HDI spatial pattern

Ordinary least squares model results

The OLS method was applied to test the principal components of the influence factors, and they all passed the test ($P<0.001$). The fit goodness, R^2, was 0.52. The AICc value was −8093.19. The variance inflation factor (VIF) values ranged from 1.02 to 3.56 (Table 6), lower than 7.5. The test indicated that they had the least redundancy and were used to analyze the spatial pattern of human disturbance in the GHMGBA ecosystems.

GWR model results

The GWR model was used to analyze the explanatory power of the five principal components. The P-values of the GWR and the OLS were less than 0.05, indicating that they were both significant. The goodness of fit, R^2, of the GWR was 0.7, which was optimized by 36.42% compared to the OLS model. The adjusted R^2 was 0.69, which was optimized by 32.69%. The AICc was −9094.22, which decreased by 1001, indicating that the GWR model fit better in this study.

The local goodness of fit, R^2, of the GWR model was 0.02–0.78 and was higher in Foshan, Guangzhou, Dongguan, and Shenzhen than that at the periphery. Only 1.43% of the grids had standardized residuals greater than 2.5. This indicated that
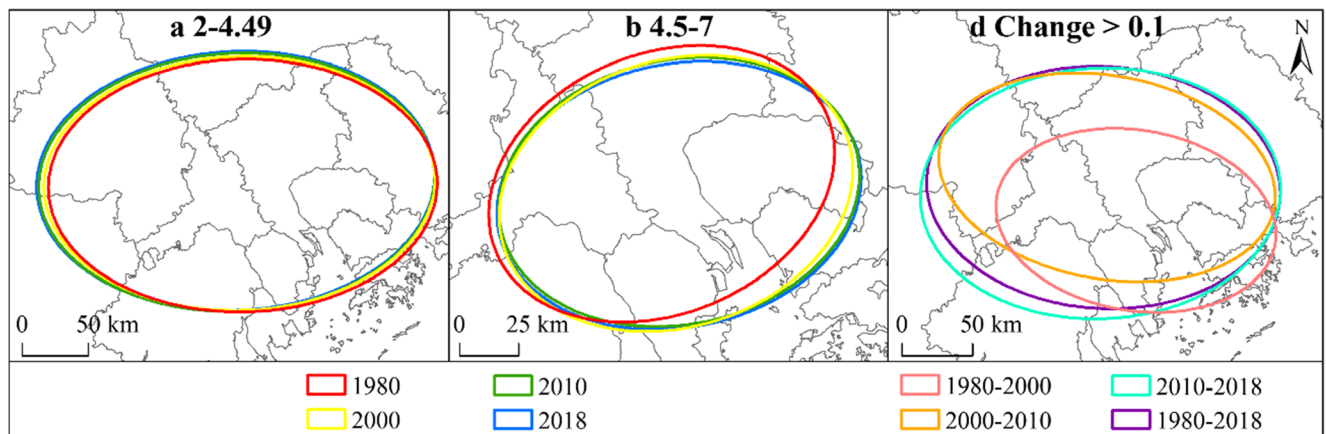
Fig. 6 Standard deviation ellipse of the HDI in the ecosystems of the GHMGBA from 1980 to 2018
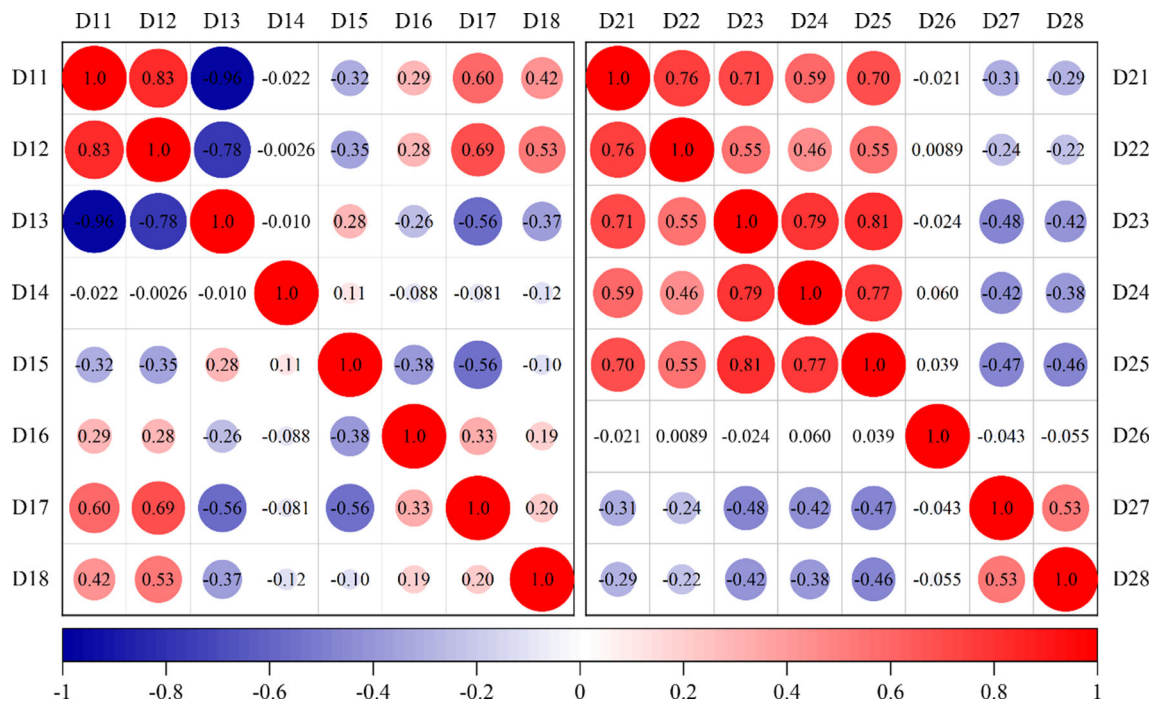
Fig. 7 Correlation analysis of the natural environmental factors (D11–D18) and social economic factors (D21–D28). D11: elevation; D12: slope; D13: annual temperature; D14: annual precipitation; D15: drainage density; D16: distance from waters; D17: NDVI; D18: farmland potential productivity; D21: population density; D22: GDP density; D23: proportion of urban land; D24: night light index; D25: traffic density; D26: ecosystem service value; D27: distance from city; D28: distance from road

98.57% of the study area had a better fit. Therefore, the GWR model was used to analyze the driving factors of the spatial pattern of the human disturbance in the GHMGBA ecosystems.

Driving factors of the HDI spatial pattern based on the GWR model

The regression coefficients of the HDI and the influencing factors from the GWR model showed obvious differences, indicating the complex characteristics of the driving factors

Table 5 Driving factors selected from the principal component score coefficient matrix

	PC-Nat 1	PC-Nat 2	PC-Nat 3		PC-Soc1	PC-Soc2
D11	0.306	−0.041	0.070	D21	0.345	−0.225
D12	0.288	−0.017	0.029	D22	0.350	−0.289
D13	−0.308	0.057	−0.112	D23	0.223	0.024
D14	0.061	−0.057	0.869	D24	0.098	0.249
D15	0.174	−0.566	−0.037	D25	0.199	0.067
D16	−0.117	0.420	−0.106	D26	−0.167	0.306
D17	0.044	0.335	0.101	D27	0.080	−0.434
D18	0.305	−0.282	−0.409	D28	0.104	−0.458

(Figure 8). The coefficients ranged from −0.8 to 0.32 for PC-Nat 1, −0.43 to 0.36 for PC-Nat 2, −0.56 to 0.7 for PC-Nat 3, −0.41 to 0.9 for PC-Soc1, and −0.14 to 0.87 for PC-Soc2. This indicated that PC-Soc1 was the primary driver of HDI change in the study area, and PC-Soc2 was secondary. These are socioeconomic factors and were higher than the three principal components of the natural environmental factors.

The role of PC-Nat1

The PC-Nat1 indicates the factors of topography, temperature, and farmland production potential. The study showed that PC-Nat1 was the primary driver among the natural environmental factors. The regression coefficients were high on the west coast of the Pearl River Delta and decreased to the periphery of the west and east (Figure 8a). The elevation and slope in the GHMGBA were low on the west coast of the Pearl River Delta, such as Foshan, Guangzhou, Zhongshan, and Zhuhai, which is the alluvial plain where the Pearl River rushes into the sea. Owing to the low and flat topography and minimal undulation, this area has been deeply disturbed by human activities. The peripheral areas, such as Zhaoqing, Jiangmen, and Huizhou, have a higher elevation than the west coast and were therefore areas with lower human disturbance. It is worth noting that Shenzhen and Hong Kong, which have high human disturbance, are characterized with higher elevations than

Table 6 Test of the selected factors using the ordinary least squares (OLS) method

Variable	Coef	StdError	t_Stat	Prob	Robust_SE	Robust_t	Robust_Pr	StdCoef	VIF
Intercept	0.37	0	137.79	0.000*	0	104.89	0.000*	0	-
PC-Nat1	0.09	0.01	7.81	0.000*	0.01	6.79	0.000*	0.16	2.14
PC-Nat 2	0.07	0.01	5.44	0.000*	0.02	3.9	0.000*	0.13	3.16
PC-Nat 3	−0.03	0	−5.25	0.000*	0	−6.98	0.000*	−0.07	1.02
PC-Soc1	0.44	0.01	30.5	0.000*	0.03	13.85	0.000*	0.61	2.13
PC-Soc2	0.17	0.01	13.08	0.000*	0.02	9.31	0.000*	0.34	3.56

*p value ($p < 0.05$)

those in the delta, and thus these areas demonstrated a significant negative correlation.

Temperature did not demonstrate an obvious spatial difference. The study area is located in a low latitude area with abundant heat from the sun, which results in no latitudinal gradient. The topography influences the temperature, with higher elevations having lower temperatures, while the lower elevations have higher temperatures and more anthropogenic heat emissions. Thus, the temperature and topography had a strong connection with each other, forming the distribution pattern shown in Figure 8a.

The farmland potential productivity was closely related to the quality and distribution of croplands. Soil development is primarily affected by the spatial patterns of climate and biological factors, which both demonstrated no obvious spatial differences in the GHMGBA. The topography influences surface moisture and sediment. Croplands with good quality soil conditions were located in the middle and lower reaches of the rivers, which belong to areas with material accumulation. These areas become the primary lands for human food production and life because of the superior natural conditions (especially sufficient water resources). Therefore, they have been deeply disturbed by human activities, with a concentrated distribution of croplands.
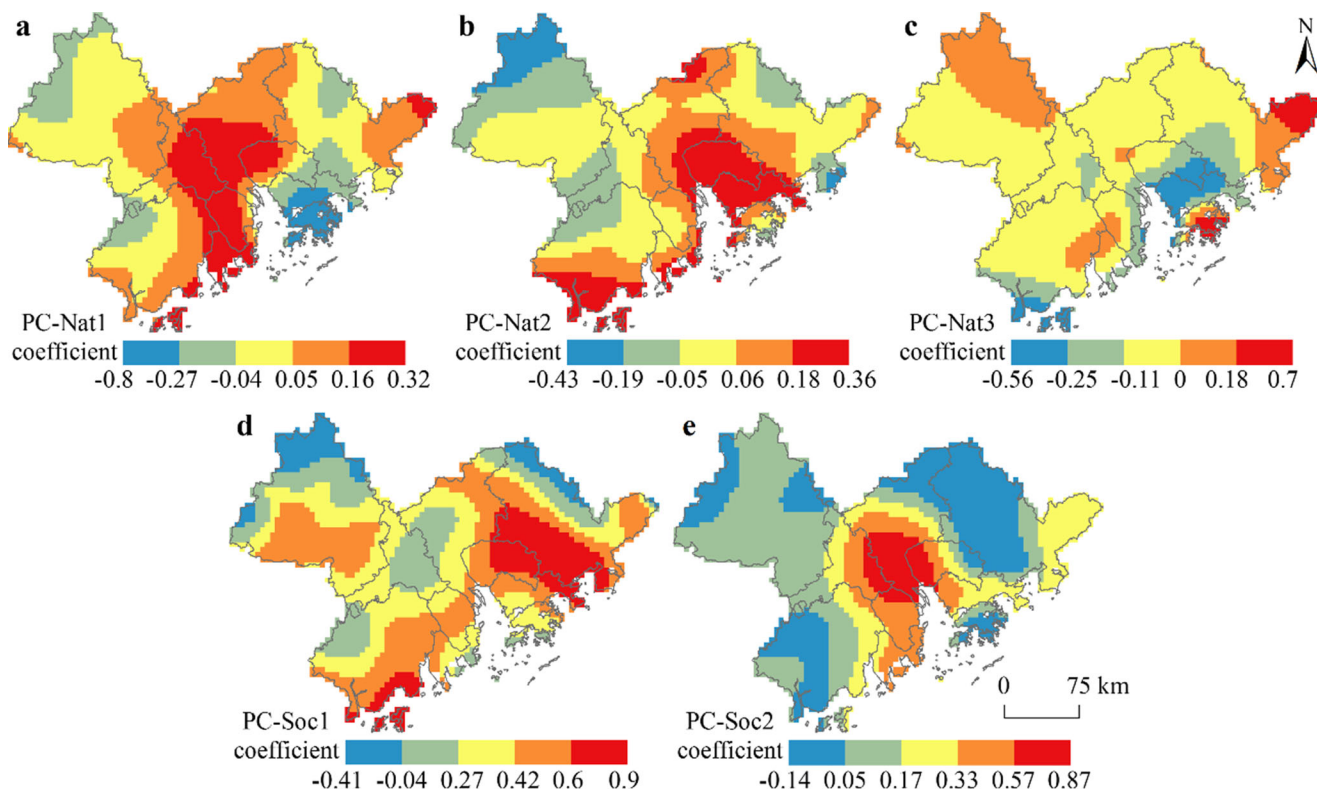
Fig. 8 Regression coefficients between the HDI and the driving factors. (a) PC-Nat1 indicates topography, temperature, and farmland potential productivity. (b) PC-Nat2 indicates water resources and vegetation conditions. (c) PC-Nat3 indicates precipitation and farmland potential productivity. (d) PC-Soc1 indicates the population, economy, and cities. (e) PC-Soc2 indicates the ecosystem service value and distances to cities and roads

The role of PC-Nat2

The regression coefficients of PC-Nat2, representing water resources and vegetation, were higher along the east coast of the Pearl River Delta and the coastal area in the southwestern area of Yangjiang and then decreased to the northwest (Figure 8b). Water resources were abundant in the lower reaches of the Pearl River and the coastal zones of the Delta, where river nets are dense and easily accessible. In addition, human disturbance is high due to intense human activities. In contrast, the northwest areas of the GHMGBA displayed low disturbance due to low human activities, and the water resources were in good condition. The PC-Nat2 had a negative relation with the HDI in this area.

The mountainous areas away from the city had low human disturbance. These areas had sufficient water and heat conditions, with high vegetation cover for the PC-Nat2. They had a negative relationship with the HDI. The riverside and seaside areas had broken landscapes and were highly influenced by man-made landscapes such as cities. The PC-Nat2 there had almost no obvious relationship with the HDI. These places included the transition zone between the core and peripheral areas and the west coast of the Pearl River Delta. Dongguan and Shenzhen had high development intensities, undulating terrains, and high vegetation cover. The PC-Nat2 in the two cities thus showed a positive correlation with the HDI.

The role of PC-Nat3

The regression coefficients of PC-Nat3, precipitation, had no obvious driving effect on the HDI in most regions, except in the southeast coast, such as Hong Kong and eastern Huizhou, where PC-Nat3 showed a significant positive correlation with the HDI. PC-Nat3 in the rest of Shenzhen and the southwest areas of the Yangjiang was negatively related to the HDI (Figure 8c). These areas have regular precipitation patterns that are higher in the northeast and southwest, decreasing to the Pearl River Delta and the lowest in the northwest. The HDI was weaker in the southwest and east and higher in the Pearl River Delta region, which showed no relationship with PC-Nat3. The southwest of Yangjiang had high precipitation and a low HDI, where PC-Nat3 had a negative correlation with the HDI. The same case was found in Shenzhen, which had moderate precipitation and a high HDI. The farmland potential productivity was described in PC-Nat1. The farmland potential productivity and HDI should be positively driven in areas with good water and soil resources near rivers, but there were obvious differences with the spatial pattern of precipitation. This leads to a less pronounced driving role for PC-Nat3.

The role of PC-Soc1

The PC-Soc1, calculated from the population, GDP, and cities, was the primary driver from the socioeconomic standpoint. Their regression coefficients were all positively correlated with the HDI in most of the regions, while negatively correlated locally only in the northwest and northeast (Figure 8d). The population, GDP, and cities had similar aggregated characteristics. Socioeconomic activities can rapidly change land cover and ecosystem structures, causing a divergence and change in the HDI. Places with large populations are economically active and prone to develop into cities. This results in high ecosystem HDIs because the settlement ecosystems expand and artificial facility utilizations increase. PC-Soc1 had a positive correlation with the HDI. The PC-Soc1 in Guangzhou and Foshan, which are the socioeconomic centers of the GHMGBA, was not obviously related to the HDI because of insufficient data spatialization. This lack of data spatialization somewhat attenuated the spatial aggregation characteristics of the population and the GDP. The economic intensity and the HDI in the junction zone of Dongguan and Huizhou were moderate, thus forming a significant positive correlation between PC-Soc1 and the HDI.

The role of PC-Soc2

The regression coefficients of PC-Soc2 from the ecosystem services value (ESV), distance to cities and roads, were annularly distribution. It was positive in the southern area of Guangzhou, eastern Foshan, northern Zhongshan, and western Dongguan, which were the centers of the correlation. It decreased to a weak negative correlation toward the periphery (Figure 8e). The ESV is closely related to the value it provides to humans. The HDI was stronger in the Pearl River Delta, which has superior resources and a higher ESV. In contrast, the HDI was lower in the surrounding areas of the GHMGBA, where the ESV is lower and the natural environment can provide relatively lower services.

The distances to cities and roads can likewise significantly reflect the spatial pattern of socioeconomic activities. The closer the cities and roads are to each other, the more significant the spatial aggregation. The Pearl River Delta region, where the indicated human activities were concentrated and the ecosystem change was obvious, suffered from a high HDI. In contrast, the peripheral areas of the GHMGBA had low HDIs. This is where the cities are far from each other and the roads are few. Hence, human activities were dispersed, and the ecosystem was less disturbed.

Discussion

Differences and similarities of human disturbance in the different studies

The human disturbance index is an empirical model that quantifies the intensity of human activities by assigning values to different surface landscape types. The idea has been adopted

by different studies. There are generally two types of disturbance level classifications. The first have decimal values from 0 to 1 that align the range of disturbance classes with the normalized range and facilitate integration with other data (Roth et al. 2016; Yi et al. 2020; Chen et al. 2020; Han et al. 2020; Wang et al. 2021). Another uses integers. Ning et al. (2015) used values from 0 to 3 and classified them into four categories. Cui et al. (2021) used values from 0 to 5 and classified them into six categories. Feng et al. (2017) and Tian et al. (2020) used values from 1 to 7 and classified them into seven categories. Zhou et al. (2018) and Yang and Song (2021) used values from 1 to 10 and divided them into 10 categories, and Tousignant et al. (2010) used values from 0 to 16 and divided them into 17 categories. Hou et al. (2019) inverted the human disturbance index, called the naturalness degree, which was also classified into seven classes.

In these studies, both the entirety of China (Ning et al. 2015), the resource-exploiting regions in North China (Tian et al. 2020), the eastern coastal zone (Zhou et al. 2018), the rapidly urbanizing coastal area and hilly regions in North China (Yi et al. 2020; Chen et al. 2020), the hilly regions in Southeast China (Han et al. 2020), and the urban agglomeration in southern China, all exhibited high levels of disturbance in urban and agricultural landscape areas. This demonstrated that despite the inconsistency in classification levels, their basic objectives were similar, and the results obtained were comparable and referable.

Influencing factors of land use change and human disturbance

Land use change in the GHMGBA and related areas has been extensively studied. It was found that the ecological carrying capacity of the region is continuing to decrease (Wang et al. 2020c), and the conversion of a large amount of natural landscape to urban land between 1980 and 2018 was an important change in the surface of GHMGBA, resulting in a loss of 4.05 billion yuan (Wang et al. 2020a). GDP, income, road length, and population are the most important drivers of urban sprawl in the GHMGBA (Zhang et al. 2020). The LUCC process is largely influenced by socioeconomic factors, leading to fragmentation of the landscape pattern (Jiao et al. 2019). In addition, ecological land also undergoes complex changes of degradation and growth, and the population density and land urbanization rate are considered as determinants, with socioeconomic factors influencing ecological land more than natural factors (Feng et al. 2021). Similarly, elevation, slope, distance from built-up land, and the growth rate of built-up land are considered important factors for ecological land conversion in Zhuhai, which is located in the southern GHMGBA (Hu and Zhang 2020).

The ecosystem and human disturbance intensity grading in this study were closely related to land use; hence, they may

have potential common influences. Wang et al. (2021) analyzed the spatially heterogeneity drivers of human disturbance in the GHMGBA land use using the geographical detectors (GeoDetector). They showed that the central major cities were significantly driven by socioeconomic activities, while the peripheral underdeveloped cities were constrained by natural environmental factors. In this study, the GWR model was used to further clarify the driving roles of the different aspects of the indicators of the natural environment and social economy in the different regions. Although the PCA results extracted more information about the natural environment, the regression coefficients of both principal components of socioeconomic factors exceeded the principal components of the natural environment. We believe that this was due to spatial heterogeneity differences in the environmental factors. Therefore, we need to pay attention to the research scale. In addition, it is suggested that the driving role of the different regions requires be further clarification, especially under different topographic conditions, such as the middle and upper reaches of the Ganjiang River Basin in hilly areas, which are also under a subtropical climate where the influence of the natural environment is more pronounced (Liu et al. 2021b).

Research deficiency and prospect

In this study, human disturbance was analyzed based on ecosystem data on long time-scale, and the influencing factors of human disturbance change were quantitatively analyzed using the GWR model. Although the driving factors were considered from the different perspectives of the natural environment and socioeconomics, the policy effects, which are difficult to quantify but have a large impact, were not considered. In addition, the impact of different land use types on human disturbances was not quantified. Therefore, subsequent studies are required to more deeply analyze these aspects.

In addition, as an important indicator for the measurement of the intensity of human activities, the human disturbance index can be used to assess ecological risk (Zhang and Chen 2014) and ecological vulnerability (Yang and Song 2021). In addition, it can be used to analyze the relationship between ecosystem services and human disturbance (Han et al. 2020), among other research directions.

Conclusion

The human disturbance intensity and its influencing factors of the ecosystem in the Guangdong-Hong Kong-Macao Greater Bay Area were analyzed in this study based on the surface landscape being defined by the human disturbance index (HDI). There were four findings. First, the HDI was divided into 6 levels and 12 categories in the GHMGBA. The spatial pattern analysis

results showed that the HDI was high in the middle and low at the periphery. Second, the human disturbance intensity increased from 1980 to 2018, during which medium and high disturbed areas greatly expanded. The concentration and direction characteristics of the HDI in the different levels showed that the standard deviation ellipse in the low HDI areas changed very little from 1980 to 2018, and moderate change took place in the high HDI areas. The standard deviation ellipse of which the HDI change more than 0.1 during the transition periods changed obviously. Third, the GWR model fit better than the OLS for analyzing the driving factors of the HDI, which had significant spatial heterogeneity. Fourth, the results of the GWR model indicated that both the positive and negative driving effects of the influencing factors on the HDI were present, but there were differences in the specific effects on different regions of the GHMGBA. Factors from the natural and socioeconomic jointly contributed to the human disturbance intensity. However, the driving effect of socioeconomic conditions was significantly stronger than that of the natural environmental, especially the population, economy, cities, ecosystem service value, and distance to cities and roads. In summary, this study quantified the human disturbance intensity of the terrestrial ecosystems of the urban agglomeration in SouthChina based on the HDI. This will assist in understanding the distribution and change characteristics of the ecological environment in areas with strong human activities. This study also provides a reference for related studies.

Author contribution Xiaojun Wang: conceptualization, methodology, and writing—original draft preparation; Guangxu Liu, Aicun Xiang, and Salman Qureshi: writing—review and editing, supervision; Tianhang Li, Dezhuo Song, and Churan Zhang: resources, data curation, and writing—original draft preparation. All authors have read and agreed to the published version of the manuscript.

Declarations

Ethical approval The authors declare that all data used in the present study were approved.

Consent to participate Not applicable

Consent to publish Not applicable

Competing interests The authors declare no competing interests.

References

Abdi H, Williams LJ (2010) Principal component analysis. Wiley Interdiscip Rev Comput Stat 2(4):433–459. https://doi.org/10.1002/wics.101

Arsiso BK, Tsidu GM, Stoffberg GH, Tadesse T (2018) Influence of urbanization-driven land use/cover change on climate: the case of Addis Ababa, Ethiopia. Phys Chem Earth 105:212–223. https://doi.org/10.1016/j.pce.2018.02.009

Asabere SB, Acheampong RA, Ashiagbor G, Beckers SC, Keck M, Erasmi S, Schanze J, Sauer D (2020) Urbanization, land use transformation and spatio-environmental impacts: analyses of trends and implications in major metropolitan regions of Ghana. Land Use Policy 96:104707. https://doi.org/10.1016/j.landusepol.2020.104707

Bi M, Xie G, Yao C (2020) Ecological security assessment based on the renewable ecological footprint in the Guangdong-Hong Kong-Macao Greater Bay Area, China. Ecol Indic 116:106432. https://doi.org/10.1016/j.ecolind.2020.106432

Chen Y, Xu N, Yu Q, Guo L (2020) Ecosystem service response to human disturbance in the Yangtze River economic belt: a case of Western Hunan, China. Sustainability 12(2):465. https://doi.org/10.3390/su12020465

Cui L, Li G, Chen Y, Li L (2021) Response of landscape evolution to human disturbances in the coastal wetlands in northern Jiangsu Province, China. Remote Sens 13(11):2030. https://doi.org/10.3390/rs13112030

Dai E, Wang Y, Ma L, Yin L, Wu Z (2018a) 'Urban-rural'gradient analysis of landscape changes around cities in mountainous regions: a case study of the Hengduan Mountain region in Southwest China. Sustainability 10(4):1019. https://doi.org/10.3390/su10041019

Dai E, Wu Z, Du X (2018b) A gradient analysis on urban sprawl and urban landscape pattern between 1985 and 2000 in the Pearl River Delta, China. Front Earth Sci 12(4):791–807. https://doi.org/10.1007/s11707-017-0637-0

de Matos SNO, Lopes LE, Costa LM, Motta-Junior JC, de Freitas GHS, Dornas T, de Vasconcelos MF, Nogueira W, de MagalhãesTolentino VC, De-Carvalho CB, Barbosa MO, Ubaid FK, Nunes AP, Malacco GB, Marini MÂ (2021) Adopting habitat-use to infer movement potential and sensitivity to human disturbance of birds in a Neotropical Savannah. Biol Conserv 254:108921. https://doi.org/10.1016/j.biocon.2020.108921

Evans IS, Robinson DT, Rooney RC (2017) A methodology for relating wetland configuration to human disturbance in Alberta. Landsc Ecol 32(10):2059–2076. https://doi.org/10.1007/s10980-017-0566-z

Feng Z, Zhang J, Hou W, Zhai L (2017) Dynamic changes of hemeroby degree based on the land cover classification: a case study in Beijing (in Chinese). Chin J Ecol 36(2):508–516. https://doi.org/10.13292/j.1000-4890.201702.028

Feng Y, Liu Y, Tong X (2018) Spatiotemporal variation of landscape patterns and their spatial determinants in Shanghai, China. Ecol Indic 87:22–32. https://doi.org/10.1016/j.ecolind.2017.12.034

Feng R, Wang F, Wang K, Xu S (2021) Quantifying influences of anthropogenic-natural factors on ecological land evolution in mega-urban agglomeration: a case study of Guangdong-Hong Kong-Macao greater Bay area. J Clean Prod 283:125304. https://doi.org/10.1016/j.jclepro.2020.125304

Fotheringham AS, Charlton ME, Brunsdon C (1998) Geographically weighted regression: a natural evolution of the expansion method

for spatial data analysis. Environ Plan A 30(11):1905–1927. https://doi.org/10.1068/a301905

Gill JA, Sutherland WJ, Watkinson AR (1996) A method to quantify the effects of human disturbance on animal populations. J Appl Ecol 33(4):786–792. https://doi.org/10.2307/2404948

Gogtay NJ, Thatte UM (2017) Principles of correlation analysis. J Assoc Physicians India 65(3):78–81 http://www.kem.edu/wp-content/uploads/2012/06/9-Principles_of_correlation-1.pdf

Gu D, Zhang Y, Fu J, Zhang X (2007) The landscape pattern characteristics of coastal wetlands in Jiaozhou Bay under the impact of human activities. Environ Monit Assess 124(1):361–370. https://doi.org/10.1007/s10661-006-9232-7

Guo S, Bai H, Meng Q, Huang X, Qi G (2018) Landscape pattern change and its response to anthropogenic disturbance in the Qinling Mountains during 1980 to 2015 (in Chinese). Chin J Appl Ecol 29(12):4080–4088. https://doi.org/10.13287/j.1001-9332.201812.018

Guo B, Wang X, Pei L, Su Y, Zhang D, Wang Y (2021) Identifying the spatiotemporal dynamic of PM2. 5 concentrations at multiple scales using geographically and temporally weighted regression model across China during 2015–2018. Sci Total Environ 751:141765. https://doi.org/10.1016/j.scitotenv.2020.141765

Han R, Feng CC, Xu N, Guo L (2020) Spatial heterogeneous relationship between ecosystem services and human disturbances: a case study in Chuandong, China. Sci Total Environ 721:137818. https://doi.org/10.1016/j.scitotenv.2020.137818

Hannah L, Lohse D, Hutchinson C, Carr JL, Lankerani A (1994) A preliminary inventory of human disturbance of world ecosystems. Ambio 23(4-5):246–250 https://www.jstor.org/stable/4314213

Hou K, Wen J (2020) Quantitative analysis of the relationship between land use and urbanization development in typical arid areas. Environ Sci Pollut Res 27(31):38758–38768. https://doi.org/10.1007/s11356-020-08577-8

Hou W, Zhai L, Qiao Q, Walz U (2019) Monitoring the intensity of human impacts on anthropogenic landscape: a mapping case study in Beijing, China. Ecol Indic 102:382–393. https://doi.org/10.1016/j.ecolind.2019.02.004

Hu Y, Zhang Y (2020) Spatial–temporal dynamics and driving factor analysis of urban ecological land in Zhuhai city, China. Sci Rep 10(1):1–15. https://doi.org/10.1038/s41598-020-73167-0

Jalas J (1955) Hemerobe und hemerochore pflanzenarten. Ein terminologischer reformversuch. Acta Soc Fauna Flora Fenn 72(11):1–15

Jiao M, Hu M, Xia B (2019) Spatiotemporal dynamic simulation of land-use and landscape-pattern in the Pearl River Delta, China. Sustain Cities Soc 49:101581. https://doi.org/10.1016/j.scs.2019.101581

Kerley LL, Goodrich JM, Miquelle DG, Smirnov EN, Quigley HB, Hornocker MG (2002) Effects of roads and human disturbance on Amur tigers. Conserv Biol 16(1):97–108. https://doi.org/10.1046/j.1523-1739.2002.99290.x

Leśniewska-Napierała K, Nalej M, Napierała T (2019) The impact of EU grants absorption on land cover changes—the case of Poland. Remote Sens 11(20):2359. https://doi.org/10.3390/rs11202359

Li J, Liu Y, Pu R, Yuan Q, Shi X, Guo Q, Song X (2018) Coastline and landscape changes in bay areas caused by human activities: a comparative analysis of Xiangshan Bay, China and Tampa Bay, USA. J Geogr Sci 28(8):1127–1151. https://doi.org/10.1007/s11442-018-1546-1

Li ZT, Li M, Xia BC (2020a) Spatio-temporal dynamics of ecological security pattern of the Pearl River Delta urban agglomeration based on LUCC simulation. Ecol Indic 114:106319. https://doi.org/10.1016/j.ecolind.2020.106319

Li Q, Zhang H, Guo S, Fu K, Liao L, Xu Y, Cheng S (2020b) Groundwater pollution source apportionment using principal component analysis in a multiple land-use area in southwestern China.

Environ Sci Pollut Res 27(9):9000–9011. https://doi.org/10.1007/s11356-019-06126-6

Liang F, Liu L (2011) Quantitative analysis of human disturbance intensity of landscape patterns and preliminary optimization of ecological function regions: a case of Minqing County in Fujian Province (in Chinese). Resour. Sci 33(6):1138–1144 http://www.resci.cn/CN/Y2011/V33/I6/1138

Liu F, Hou H, Murayama Y (2021a) Spatial interconnections of land surface temperatures with land cover/use: a case study of Tokyo. Remote Sens 13(4):610. https://doi.org/10.3390/rs13040610

Liu G, Wang X, Xiang A, Wang X, Wang B, Xiao S (2021b) Spatial heterogeneity and driving factors of land use change in the middle and upper reaches of Ganjiang River, southern China (in Chinese). Chin J Appl Ecol 32(7):2545–2554. https://doi.org/10.13287/j.1001-9332.202107.016

Ma Y, Zhang S, Yang K, Li M (2021) Influence of spatiotemporal pattern changes of impervious surface of urban megaregion on thermal environment: a case study of the Guangdong-Hong Kong-Macao Greater Bay Area of China. Ecol Indic 121:107106. https://doi.org/10.1016/j.ecolind.2020.107106

Mansour S, Al-Belushi M, Al-Awadhi T (2020) Monitoring land use and land cover changes in the mountainous cities of Oman using GIS and CA-Markov modelling techniques. Land Use Policy 91:104414. https://doi.org/10.1016/j.landusepol.2019.104414

Markovchick-Nicholls LISA, Regan HM, Deutschman DH, Widyanata A, Martin B, Noreke L, Ann Hunt T (2008) Relationships between human disturbance and wildlife land use in urban habitat fragments. Conserv Biol 22(1):99–109. https://doi.org/10.1111/j.1523-1739.2007.00846.x

Ning J, Liu J, Zhao G (2015) Spatio-temporal characteristics of disturbance of land use change on major ecosystem function zones in China. Chin Geogr Sci 25(5):523–536. https://doi.org/10.1007/s11769-015-0776-8

Pei L, Wang X, Guo B, Guo H, Yu Y (2021) Do air pollutants as well as meteorological factors impact corona virus disease 2019 (COVID-19)? Evidence from China based on the geographical perspective. Environ Sci Pollut Res 28:35584–35596. https://doi.org/10.1007/s11356-021-12934-6

Peng J, Tian L, Liu Y, Zhao M, Wu J (2017) Ecosystem services response to urbanization in metropolitan areas: thresholds identification. Sci Total Environ 607:706–714. https://doi.org/10.1016/j.scitotenv.2017.06.218

Peng T, Sun C, Feng S, Zhang Y, Fan F (2021) Temporal and spatial variation of anthropogenic heat in the central urban area: a case study of Guangzhou, China. ISPRS Int J Geo-Inf 10(3):160. https://doi.org/10.3390/ijgi10030160

Propastin P (2012) Modifying geographically weighted regression for estimating aboveground biomass in tropical rainforests by multispectral remote sensing data. Int J Appl Earth Obs Geoinf 18:82–90. https://doi.org/10.1016/j.jag.2011.12.013

Qin Y, Ren G, Huang Y, Zhang P, Wen K (2021) Application of geographically weighted regression model in the estimation of surface air temperature lapse rate. J Geogr Sci 31(3):389–402. https://doi.org/10.1007/s11442-021-1849-5

Qureshi S, Alavipanah SK, Konyushkova M, Mijani N, Fathololomi S, Firozjaei MK, Homaee M, Hamzeh S, Kakroodi AA (2020) A remotely sensed assessment of surface ecological change over the Gomishan Wetland, Iran. Remote Sens 12(18):2989. https://doi.org/10.3390/rs12182989

Ren Y, Deng L, Zuo S, Luo Y, Shao G, Wei X, Hua L, Yang Y (2014) Geographical modeling of spatial interaction between human activity and forest connectivity in an urban landscape of southeast China. Landsc Ecol 29(10):1741–1758. https://doi.org/10.1007/s10980-014-0094-z

Roth D, Moreno-Sanchez R, Torres-Rojo JM, Moreno-Sanchez F (2016) Estimation of human induced disturbance of the environment

associated with 2002, 2008 and 2013 land use/cover patterns in Mexico. Appl Geogr 66:22–34. https://doi.org/10.1016/j.apgeog.2015.11.009

Shi H, Lu J, Zheng W, Sun J, Li J, Guo Z, Huang J, Yu S, Yin L, Wang Y, Ma Y, Ding D (2020) Evaluation system of coastal wetland ecological vulnerability under the synergetic influence of land and sea: a case study in the Yellow River Delta, China. Mar Pollut Bull 161:111735. https://doi.org/10.1016/j.marpolbul.2020.111735

Stankowich T (2008) Ungulate flight responses to human disturbance: a review and meta-analysis. Biol Conserv 141(9):2159–2173. https://doi.org/10.1016/j.biocon.2008.06.026

Sukopp H (1976) Dynamik und Konstanz in der flora der Bundesrepublik Deutschland. Schriftenreihe fur Vegetationskunde 10:9–27

Tian Y, Liu B, Hu Y, Xu Q, Qu M, Xu D (2020) Spatio-temporal land-use changes and the response in landscape pattern to hemeroby in a resource-based city. ISPRS Int J Geo-Inf 9(1):20. https://doi.org/10.3390/ijgi9010020

Tousignant MÊ, Pellerin S, Brisson J (2010) The relative impact of human disturbances on the vegetation of a large wetland complex. Wetlands 30(2):333–344. https://doi.org/10.1007/s13157-010-0019-9

Walz U, Stein C (2014) Indicators of hemeroby for the monitoring of landscapes in Germany. J Nat Conserv 22(3):279–289. https://doi.org/10.1016/j.jnc.2014.01.007

Wang G, Liao S (2006) Spatial heterogeneity of land use intensity (in Chinese). Chin J Appl Ecol 17(4):611–614. https://doi.org/10.13287/j.1001-9332.2006.0124

Wang R, Xu T, Yu L, Zhu J, Li X (2013) Effects of land use types on surface water quality across an anthropogenic disturbance gradient in the upper reach of the Hun River, Northeast China. Environ Monit Assess 185(5):4141–4151. https://doi.org/10.1007/s10661-012-2856-x

Wang Y, Dai E, Yin L, Ma L (2018) Land use/land cover change and the effects on ecosystem services in the Hengduan Mountain region, China. Ecosyst Serv 34:55–67. https://doi.org/10.1016/j.ecoser.2018.09.008

Wang X, Yan F, Su F (2020a) Impacts of urbanization on the ecosystem services in the Guangdong-Hong Kong-Macao Greater Bay Area, China. Remote Sens 12(19):3269. https://doi.org/10.3390/rs12193269

Wang Z, Xiao J, Wang L, Liang T, Guo Q, Guan Y, Rinklebe J (2020b) Elucidating the differentiation of soil heavy metals under different land uses with geographically weighted regression and self-organizing map. Environ Pollut 260:114065. https://doi.org/10.1016/j.envpol.2020.114065

Wang YN, Zhou Q, Wang HW (2020c) Assessing ecological carrying capacity in the Guangdong-Hong Kong-Macao Greater Bay Area based on a three-dimensional ecological footprint model. Sustainability 12(22):9705. https://doi.org/10.3390/su12229705

Wang X, Zhang C, Liao Y, Liu G, Wang B, Yu J (2021) Spatial and temporal characteristics of hemeroby in Guangdong-Hong Kong-Macao Greater Bay area during 1980-2018 (in Chinese). Bull. Soil Water Conserv. 41(3):333–341. https://doi.org/10.13961/j.cnki.stbctb.2021.03.011

Weng H, Kou J, Shao Q (2020) Evaluation of urban comprehensive carrying capacity in the Guangdong–Hong Kong–Macao Greater Bay Area based on regional collaboration. Environ Sci Pollut Res 27(16):20025–20036. https://doi.org/10.1007/s11356-020-08517-6

Wu W, Zhao S, Zhu C, Jiang J (2015) A comparative study of urban expansion in Beijing, Tianjin and Shijiazhuang over the past three decades. Landsc Urban Plan 134:93–106. https://doi.org/10.1016/j.landurbplan.2014.10.010

Xu M, Zhang Z (2021) Spatial differentiation characteristics and driving mechanism of rural-industrial land transition: a case study of Beijing-Tianjin-Hebei region, China. Land Use Policy 102:105239. https://doi.org/10.1016/j.landusepol.2020.104958

Xu Q, Yang R, Zhuang D, Lu Z (2021) Spatial gradient differences of ecosystem services supply and demand in the Pearl River Delta region. J Clean Prod 279:123849. https://doi.org/10.1016/j.jclepro.2020.123849

Yang Y, Song G (2021) Human disturbance changes based on spatiotemporal heterogeneity of regional ecological vulnerability: a case study of Qiqihaer city, northwestern Songnen Plain, China. J Clean Prod 291:125262. https://doi.org/10.1016/j.jclepro.2020.125262

Yi L, Qian J, Kobuliev M, Han P, Li J (2020) Dynamic evaluation of the impact of human interference during rapid urbanisation of coastal zones: a case study of Shenzhen. Sustainability 12(6):2254. https://doi.org/10.3390/su12062254

Yu Z, Yao Y, Yang G, Wang X, Vejre H (2019) Spatiotemporal patterns and characteristics of remotely sensed region heat islands during the rapid urbanization (1995–2015) of southern China. Sci Total Environ 674:242–254. https://doi.org/10.1016/j.scitotenv.2019.04.088

Zhai L, Zhang N, Hou W, Feng Z, Qiao Q, Luo M (2018) From big data to big analysis: a perspective of geographical conditions monitoring. Int J Image Data Fusion 9(3):194–208. https://doi.org/10.1080/19479832.2018.1482965

Zhang H, Chen L (2014) Using the ecological risk index based on combined watershed and administrative boundaries to assess human disturbances on river ecosystems. Hum Ecol Risk Assess 20(6):1590–1607. https://doi.org/10.1080/10807039.2013.842746

Zhang J, Yu L, Li X, Zhang C, Shi T, Wu X, Yang C, Gao W, Li Q, Wu G (2020) Exploring annual urban expansions in the Guangdong-Hong Kong-Macau Greater Bay Area: spatiotemporal features and driving factors in 1986–2017. Remote Sens 12(16):2615. https://doi.org/10.3390/rs12162615

Zhou Y, Ning L, Bai X (2018) Spatial and temporal changes of human disturbances and their effects on landscape patterns in the Jiangsu coastal zone, China. Ecol Indic 93:111–122. https://doi.org/10.1016/j.ecolind.2018.04.076

Zhou R, Lin M, Gong J, Wu Z (2019) Spatiotemporal heterogeneity and influencing mechanism of ecosystem services in the Pearl River Delta from the perspective of LUCC. J Geogr Sci 29(5):831–845. https://doi.org/10.1007/s11442-019-1631-0

Zhuang D, Liu J (1997) Study on the model of regional differentiation of land use degree in China (in Chinese). J. Nat. Resour 12(2):105–111. https://doi.org/10.11849/zrzyxb.1997.02.002